Published in final edited form as:
Adv Healthc Mater. 2014 August ; 3(8): 1272–1282. doi:10.1002/adhm.201300696.

Particle-stabilized emulsion droplets for gravity-mediated targeting in the posterior segment of the eye

Yoo C Kim, PhD,
School of Chemical and Biomolecular Engineering Georgia Institute of Technology 311 Ferst Drive NW Atlanta, GA, 30332 uchunkim@gatech.edu

Henry F Edelhauser, PhD*, and
Department of Ophthalmology Emory University School of Medicine 1365 Clifton Rd NE Atlanta, GA, 30322

Mark R Prausnitz, PhD*
School of Chemical and Biomolecular Engineering Georgia Institute of Technology 311 Ferst Drive NW Atlanta, GA, 30332

Abstract

This study tested the hypothesis that high-density particle-stabilized emulsion droplets (PEDs) can be designed to use gravity to target specific locations in the eye via suprachoroidal space injection. PEDs contained a core of high-density perfluorodecalin measuring ≤35 μm in diameter surrounded and stabilized by fluorescein-tagged, polystyrene nanoparticles that simulated polymeric drug carriers. A hollow microneedle infused PEDs into the suprachoroidal space of rabbit eyes in vivo, which were later dissected and imaged to quantify distribution of fluorescent nanoparticles within the suprachoroidal space. With cornea oriented upward, such that gravity should move PEDs toward the back of the eye, up to 50% of nanoparticles were in the most posterior quadrant near the macula immediately after injection and five days later. With cornea oriented downward, to promote PED movement toward the front of the eye, approximately 60% of injected nanoparticles were targeted to the most anterior quadrant of the posterior segment near ciliary body. Injection of approximately neutral-density particles of the same size showed approximately equal distribution throughout the posterior segment. This study demonstrates for the first time that high-density PEDs can be used to deliver nanoparticles to specific locations in the back of the eye, including targeted delivery to the macula.

Keywords

microneedle; ophthalmic drug delivery; particle-stabilized emulsion droplet; posterior segment of the eye; and suprachoroidal space

*ophthfe@emory.eduprausnitz@gatech.edu.

Supporting Information
Supporting Information is available from the Wiley Online Library or from the author.

1. Introduction

Age-related macular degeneration (AMD) is the third leading cause of blindness worldwide. It is estimated that more than 1.8 million individuals in the United States are afflicted by wet AMD, and that number is expected to grow to almost 3 million by 2020[1]. Within the past decade, a number of new therapeutic agents have become available to mange chorioretinal diseases like AMD, as well as diabetic retinopathy, uveitis and other sight-threatening diseases[2]. However, there are no clinically used methods to target delivery of drugs specifically to their site of action within the eye to further optimize treatment efficacy.

Currently, drugs used to treat chorioretinal diseases are typically administered by intravitreal injection, which involves injection into the vitreous humor in the center of the eye using a hypodermic needle. In some cases, sustained-release formulations are delivered as an implant that is placed in the vitreous humor. However, the site of drug action is not located in the vitreous humor but in the retina or choroid instead[3]. In the case of AMD, the treatment site is at the macula, which is located in the very back of the eye near the optic nerve[4]. Using these conventional methods, drug delivered to the vitreous humor diffuses over time throughout the eye, such that a portion of the drug reaches it therapeutic target. However, drug also reaches off-target sites, which can cause side effects. For example, intravitreal administration of steroids causes unwanted contact with the lens and promotes formation of cataracts in 7 - 29% of patients[5]. In addition, administration of sustained-release formulations can require surgical procedures to insert the implants. To overcome these limitations, a new delivery method is needed that can administer pharmacotherapies to the retina and choroid in the back of the eye, including specifically targeting the macula for treatment of AMD. .

Drug targeting within the eye to treat AMD, glaucoma and other diseases can be accomplished by administering drugs into the suprachoroidal space[6]. The suprachoroidal space is a potential space located between sclera and choroid that can expand to accommodate a fluid or drug formulation. Injection of a drug formulation throughout the suprachoroidal space delivers drug directly to the choroid and adjacent retina in a more targeted manner than intravitreal injection. Delivery to the most posterior portion of the suprachoroidal space can target the macula, which is of interest for treatment of AMD. Delivery to the most anterior portion of the suprachoroidal space can target the ciliary body, which is of interest for treatment of glaucoma. For this reason, the suprachoroidal space represents a promising new site of administration for treatment many ocular diseases. However it is difficult to access the suprachoroidal space. Prior methods have involved surgical techniques[7, 8].

Recently, we introduced the use of microneedles to inject drug formulations into the suprachoroidal space in a minimally invasive manner[6, 9]. These microneedles are 30- to 33-gauge hypodermic needles that have been laser-machined to a length of less than 1 mm, which allows them to cross the sclera and overlying conjunctiva for precise placement of the needle tip at the suprachoroidal space. This injection procedure, which requires minimal training for an experienced researcher or ophthalmologist, has been used extensively in animals[6, 9, 10, 11] and, more recently, in human subjects[12]. Upon fluid injection, the

suprachorodal space can expand to incorporate injected materials, including polymeric particle formulations[9]. Injection of unformulated particles in saline distributes the particles over a portion of the suprachorodial space, but does not target delivery to specific regions within suprachoroidal space[13].

To improve on this technique, in this study we developed a new formulation to deliver nanoparticles to specific sites within the suprachoroidal space using emulsion droplets to target the macula near the back of the suprachoroidal space and to target the ciliary body near the front of the suprachoroidal space. These particle-stabilized emulsion droplets (PEDs) have high-density perflurodecalin liquid at their core and are stabilized around the edges using nanoparticles. Perfluorodecalin has approximately twice the density of water and this density difference is used to move these particles within the suprachoroidal space in the direction of gravity. The nanoparticles have a dual purpose of carrying encapsulated drugs and stabilizing the emulsion droplets, using the approach of a Pickering emulsion[14, 15]. We believe this is the first study to target particles to specific locations in the back of the eye via the suprachoroidal space.

The idea of using gravity and density differences to enhance targeting of particles has been studied before, for example, with low-density particles that float in the stomach to enhance gastric retention or that fly through the airways of the lung to facilitate pulmonary delivery[16, 17]. Our approach and these prior approaches are similar in that the key parameter is density difference between the particles and their carrier fluid. However, to our knowledge, this is first study of high-density emulsions for ophthalmic drug delivery to the posterior of the eye. We examined the design and performance of PEDs inside the suprachoroidal space. Overall, this study shows that gravity-mediated delivery using PEDs can provide targeted administration of nanoparticles near the macula or ciliary body using a minimally invasive microneedle device.

2. Results

2.1. Fabrication and characterization of particle-stabilized high-density emulsion droplets (PEDs)

This project was guided by three design criteria. First, we wanted to design a particle that could be targeted to the back of the posterior segments of the eye near the macula (for possible treatment of AMD) and to the front of the posterior segment of the eye near the ciliary body and trabecular meshwork (for possible treatment of glaucoma). Our approach to meeting this criterion was to administer high-density particles into the suprachoroidal space. Second, we wanted these particles to have the ability to slowly release drug over time, so that the particles could be injected into the eye infrequently (e.g., at doctor's office visits) and provide therapy for an extended time. To meet this criterion, we envision using biodegradable polymer particles that are well established in the literature for controlled release of encapsulated drugs. Third, we wanted the particles to be biocompatible for safe use in the eye.

We developed high-density PEDs to meet these three criteria (**Figure 1a**). The particles contain a high-density core of perfluorodecalin (1.9 g cm^{-3}), which should promote their

settling to the back or front of the eye, depending on the orientation of the eye relative to gravity (**Figure 1b – 1e**). Perfluorodecalin is widely used in vitreoretinal surgery and therefore has a well-established safety record in the eye[18].

Because perfluorodecalin is not well suited for controlled release of drugs, we stabilized the interface of the perfluorodecalin emulsion droplets using polymeric nanoparticles. We envision in the future using nanoparticles made out of a biodegradable polymer (e.g., polylactic-co-glycolic acid) encapsulating a drug for controlled release. However, for this initial study, we used polystyrene particles labeled with red-fluorescent dye as a model system to easily trace and quantify targeting efficiency of the injected PEDs. In this way, the polymeric nanoparticles served two functions: stabilizing the emulsion interface to prevent coalescence into larger droplets (i.e., by forming a Pickering emulsion[14, 15]) and providing a future means for controlled release of encapsulated drugs.

Stabilization of the emulsion droplets was achieved by controlling two properties of the polymeric nanoparticles. First, the hydrophilicity was controlled such that the nanoparticles prefer to be at the emulsion droplet interface and not in either the surrounding water or the perfluorodecalin core[19]. We therefore used polystyrene particles modified with carboxylate groups on the surface, which provided a zeta potential of -47.5±6.07mV. Second, we sought to use the largest possible polymer nanoparticles, since larger particles generally enable longer controlled release. We found that nanoparticles up to 200 nm in diameter could be used, but we failed to create emulsion droplets using larger nanoparticles (data not shown).

Next, we wanted to make PEDs as large as possible to promote rapid settling in the eye due to gravity. We varied PED size by varying the concentration of nanoparticles in the solution when fabricating the PEDs. As shown in **Figure S1a** (see Supplemental Information), PED size decreased with increasing nanoparticle concentration, which is consistent with observations by others[20]. Increased nanoparticle concentration allows larger surface area coverage of the emulsion droplets, which results in smaller size of PEDs (i.e., higher surface-to-volume ratio). Because PED populations produced in this way were highly poly-disperse (see **Figure S1b**), we prepared more uniform particle size distributions by separating the PEDs into size fractions by passing sequentially through nylon net membrane filters of 11, 20, 30 and 40 μm pore size, which produced PED populations of 14 ± 4.3 μm, 25 ± 6.0 μm and 35 ± 7.5 μm diameter (**Figures 2a-2c**). The ability to separate the different PED sizes by filtration shows that the PEDs were mechanically strong enough to withstand the separation process.

As shown in **Figure 2**, each PED contained a non-fluorescent interior composed of perfluorodecalin and a film of red-fluorescent nanoparticles around the outer surface. The high-density of the PEDs was demonstrated by rapid settling under gravity, as shown in **Figure 2d**. PEDs were designed to fall quickly in the eye due to gravity, with the expectation that larger particles should fall faster than smaller particles due to their increased mass. To determine the fall time of the PEDs in water, which provides an initial estimate of fall time inside the eye after injection, experimental measurements and theoretical calculations were performed. The measured time for PEDS of 14 μm, 25 μm and 35 μm diameter to fall to the bottom of a vial filled with water to a height of 1 cm was 93±3 s, 54±5

s, and 31±2.4 s, respectively (**Figure S2** in Supplemental Information). A simple force balance to model the process predicted fall times of 104 s, 32 s and 16 s, respectively. The discrepancies between measured and calculated values may be due to variation of the size of and interaction between the PEDs, as well as the subjective nature of experimentally determining when all PEDs settled to the bottom by visualization. In any case, settling times by measurement and calculation were fast, i.e., on the order of 1 min.

2.2. Use of gravity to target PEDs within the rabbit eye ex vivo

Before conducting *in vivo* experiments, we tested our hypothesis that deposition of PEDs in eye can be directed by gravity by injecting 35 μm-diameter PED suspensions in the suprachoroidal space of the rabbit eye *ex vivo* and changing orientation of the eye with respect to gravity. We used 35 μm-diameter PEDs because of its faster fall time compared to smaller PEDs (see below). We first targeted delivery to the anterior portion of the suprachoroidal space by positioning the eye with the cornea facing down and injecting a suspension of PEDs into the suprachoroidal space using a microneedle. The distribution of PEDs after injection was determined by dividing the suprachoroidal space into four antero-posterior quadrants (**Figure S4** in Supplemental Information). We found that 59% of the injected PEDs were targeted to the most anterior quadrant, located between the ciliary body and the site of injection 3 mm back from the ciliary body, and 85% were located in the two most anterior quadrants (i.e., < 6 mm from the ciliary body) (**Figure 3b and 3d**). Particle concentration decreased further back in the eye, with just 2.3% of PEDs in the most posterior quadrant located 9 mm or further back from the ciliary body. There was a statistically significant decrease in PED concentration moving posteriorly within the suprachoroidal space (one-way ANOVA, $p = 0.0002$). This shows significant targeting of the PEDs to the anterior portion of the suprachoroidal space.

We next targeted delivery to the posterior portion of the suprachoroidal space by positioning the eye with the cornea facing up. In this case, 30% of the injected PEDs were located in the most posterior quadrant adjacent to the macula and 61% were loaded in the two most posterior quadrants (> 6 mm from the ciliary body) (**Figure 3c and 3d**). Just 9.6% were in the most anterior quadrant. There was a statistically significant increase in PED concentration moving posteriorly within the first three quadrants of the suprachoroidal space (one-way ANOVA, $p = 0.02$). This shows significant targeting of the PEDs to the posterior portion of the suprachoroidal space and, when compared with the anteriorly targeted data, demonstrates the gravity-mediated mechanism of the targeting.

Finally, we were interested to characterize the radial distribution of PEDS to the left and right of the injection site. As shown in **Figure 3e**, the large majority of the particles were located in the upper radial quadrants immediately to the left and right of the injections site (i.e., between -90° to 0° and 0° to 90°) and very little reached the lower radial quadrants (i.e., between -180° to -90° and 90° to 180°). There was no significant difference between the particle concentrations in each of these quadrants as a function of eye orientation (i.e., cornea up versus cornea down, $p > 0.10$). This is expected, because radial movement is in the direction perpendicular to the gravitational field, meaning that gravity should not influence radial movement.

2.3. Use of gravity to target PEDs within the rabbit eye *in vivo*

Next, we repeated the injection of 35 μm PEDs into the rabbit eye *in vivo* to determine if *ex vivo* results can be translated to *in vivo* eyes. The distribution of PEDs in each antero-posterior quadrant of the suprachoroidal space after injection *in vivo* was not significantly different from injection *ex vivo* (one-way ANOVA, $p > 0.7$, see **Figure S3** in Supplemental Information). The radial distributions for *in vivo* and *ex vivo* eyes also showed no significant differences (one-way ANOVA, $p > 0.8$). These data show a good correlation between *ex vivo* and *in vivo* injections and demonstrate the use of gravity to target PEDs within the living rabbit eye.

Our central hypothesis is that the use of PEDs with a density greater than water enables gravity-mediated targeting. Therefore, to further assess the role of gravity to target movement of PEDs inside the suprachoroidal space, we carried out an identical experiment *ex vivo* using fluorescently tagged polystyrene microparticles with a 32 μm diameter that were almost neutral density compared to water (1.05 g-cm^{-3}) and compared them to PEDs with a 35 μm diameter containing high-density perflurodecalin (1.92 g-cm^{-3}). The injection conditions in both cases were the same, such as volume injected (200 μL), concentration of particles (5% by volume) and cornea facing up. As shown in **Figure 4**, injection of the neutral-density polystyrene fluorescent microparticles resulted in just 13±5% of the particles reaching the most posterior quadrant. In contrast, 2.5 times more of the high-density PEDs reached the most posterior quadrant (i.e., 32±12%). One-way ANOVA analysis shows a statistically significant increase in PED concentration moving posteriorly within the first three quadrants of the suprachoroidal space (one-way ANOVA, $p = 0.0020$). In contrast, there was no statistically significant change in concentration of the polystyrene microparticles within the first three antero-posterior quadrants (one-way ANOVA, $p = 0.99$). The radial distributions showed no significant differences (one-way ANOVA, $p > 0.10$) between PEDs and polystyrene microparticles.

2.4. Retention of PEDs at the site of targeted delivery

To be most valuable, PEDs should not move around inside the eye after the targeted injection. We hypothesized that the suprachoroidal space expands during an injection but collapses back to its normal position as fluid dissipates and that this collapse will immobilize the PEDs. To test this hypothesis, we injected PEDs into the left-side eyes of rabbits *in vivo* with the cornea facing up to localize PEDs to the back of the eye. After five days, during which time the rabbits were allowed to move freely, we performed identical injections into the right-side eyes and then immediately sacrificed the animals to compare PED distribution immediately after and five days after injection. As shown in **Figure 5**, the distribution of PEDs in both cases showed a similar trend of increasing PED content toward the back of the eye. After five days, 50% of the injected PEDs were located in the most posterior quadrant adjacent to the macula and 77% were loaded in the two most posterior quadrants (> 6 mm from the ciliary body) (**Figure. 5c**). Statistical analysis (one-way ANOVA) between antero-posterior tissue segments in the two groups were not significant different ($p>0.01$), except in the 6 – 9 mm segment ($p = 0.032$). The radial distributions for eyes at 0 days and 5 days after injection showed no significant differences (one-way ANOVA, $p > 0.25$). We therefore conclude that PEDs can be targeted to regions of the

suprachoroidal space during injection and then can be retained at the site of targeted delivery afterwards. Additional studies will be needed to further assess this retention of PEDs over longer times and, eventually, in humans.

2.5. Effect of PED size on gravity-mediated targeting

As a further test of gravity-mediated delivery, we sought to measure the mobility of PEDs inside the suprachoroidal space as a function of PED size, with the expectation that larger PEDs should be better targeted by gravity due to their faster fall time (see **Figure S2**). We therefore injected PEDs of 14 μm, 25 μm and 35 μm diameter (see **Figure 2**) into the suprachoroidal space and measured the extent of posterior targeting with the cornea facing up in the rabbit eye in vivo. As shown in **Figure 6**, PED concentration increased significantly when moving posteriorly within the first three quadrants of the suprachoroidal space for the 35 μm PEDs (one-way ANOVA, $p = 0.002$), but not for the smaller PEDs (one-way ANOVA, $p > 0.81$). This suggests that 35 μm PEDs are optimal for gravity-mediated targeting among the PED sizes tested. It is possible that still-larger PEDS would provide even better targeting by gravity. However, if the PEDs become too large their movement in the suprachoroidal space and in the microneedle during injection may be hindered.

2.6. Kinetics of suprachoroidal space collapse

An important parameter that could affect the movement of PEDs in the suprachoroidal space is the time it takes for the suprachoroidal space to collapse after the injection and thereby prevents further movement of the PEDs. Because larger particles were able to more effectively target the back of the eye (**Figure 6**) and because these particles have a 1-cm fall time on the order of 1 min (**Figure 2**), we hypothesize that the suprachoroidal space collapses on a similar timescale on the order of 1 min.

To test this hypothesis, we determined the time it takes for fluid to dissipate from the suprachoroidal space by two methods. First, we measured intraocular pressure (IOP) over time after injection as an indirect measure of suprachoroidal space expansion. As shown in **Figure 7a**, IOP increased by 72 mm Hg upon injection, substantially dropped within 5 min and then returned to baseline IOP within 20 min. The initial increase in IOP is believed to be due to introduction of additional fluid into the eye. This effect is seen after intravitreal injection as well[21]. The decay in IOP is believed to be due to clearance of the fluid from the eye. These data therefore suggest that fluid that is injected into the suprachoroidal space is largely cleared from the eye within 5 min and completely within 20 min. This measurement may provide an overestimate of the time for suprachoroidal space collapse, because fluid in the suprachoroidal space may first redistribute within the eye (which could collapse the suprachoroidal space, but not reduce IOP) and then be cleared from the eye (which would reduce IOP).

The second method we used to assess the kinetics of suprachoroidal space collapse employed ultrasound imaging to directly measure the height of the suprachoroidal space over time at a single location. Measurements by ultrasound at a location 45° away radially from the injection site showed immediate expansion of the suprachoroidal space to as much

as ~1000 μm spacing, followed by substantial collapse within tens of seconds. We believe that this more direct measurement provides a more accurate estimate of suprachoroidal space collapse time. This rapid collapse of the suprachoroidal space could explain why 35 μm PEDs showed better movement towards the back of the eye compared to smaller PEDs (**Figure 6**).

3. Discussion

While most efforts to target drug delivery for ocular applications seek to preferentially deliver drugs to the eye as opposed to other parts of the body, more recent efforts have emphasized more-precisely targeted delivery that directs drug delivery within the eye to specific sites of drug action. In this study, we leveraged previous work that has demonstrated delivery targeted to the suprachoroidal space[6, 7, 9, 11] and added to it the ability to direct delivery within the suprachoroidal space to target the very back of the eye for possible treatment of AMD and other disorders of the macula or the anterior portion of the suprachoroidal space for possible treatment of glaucoma with sites of action in the ciliary body or trabecular meshwork. To our knowledge, this is the first study to actively direct movement of particles within the suprachoroidal space for targeted delivery.

Targeting was achieved in this study through the use of high-density PEDs that could be moved by gravity. The design of PEDs achieved gravity-mediated delivery using a perfluorodecalin core stabilized with polymeric nanoparticles that could be adapted in the future for controlled release of encapsulated drugs. Perfluorodecalin was chosen as the core material not only because of its high density, but also because it has been safely used in vitreoretinal surgery for decades[18] [22] and other similar perfluorocarbons are widely used for clinic imaging applications[23]. While we chose to use liquid perfluorodecalin to provide high density and solid polymer nanoparticles to provide future controlled release functionality, alternative designs might choose different materials or combinations of materials to achieve these two capabilities.

PEDs were stabilized in this study using polymeric nanoparticles. Stabilizing emulsion droplet using solid particles has been known since Pickering[14] originally recognized the role of solid particles in stabilizing emulsions. Such Pickering emulsions have found many uses in the food, cosmetic, pharmaceutical, petroleum, and agricultural industries[24], as well as for applications in triggered drug delivery[25].

The idea of using particle density to facilitate targeted drug delivery has been used before in other contexts. One example is low-density, porous particles that follow air stream lines such that the particles are designed to flow with their carrier fluid of air and thereby enhance pulmonary delivery deep in the lung[17, 26]. Another example involves creating low-density particles that float in stomach fluid such that the particles are designed not to flow with their carrier fluid of stomach juices and thereby enhance gastric retention[27]. This study differs from these previous studies in that we used high-density particles to facilitate directed movement through a largely static carrier fluid in the suprachoroidal space.

For possible future clinical use of PEDs for targeted drug delivery in the eye, we envision patients lying down on an exam table (either face up or face down, depending on whether posterior or anterior targeting is needed) for a period of time after receiving an injection to let the PEDs move to their target location while the suprachoroidal space collapses.

We believe that suprachoroidal injection of PEDs can be done safely and reliably. In current clinical practice, retina specialists give millions of intravitreal injections per year by inserting a hypodermic needle across the pars plana of the eye into the middle of the eye[28]. Suprachoroidal injection requires placement of a microneedle at the same site and making a much shallower injection at the base of the sclera. The depth of this injection is controlled by microneedle length, which can be matched to scleral thickness. Microneedles have been reliably used and well tolerated in hundreds of suprachoroidal injections in rabbits, in pigs and recently in human subjects[6, 9, 11, 12].

4. Conclusion

This study developed high-density PED particles for gravity-mediated targeting in the posterior segment of the eye. The design of these PED particles features a core of perfluorodecalin, which is a high-density liquid droplet made of a biocompatible material widely used in the eye, surrounded by polymeric nanoparticles coating the droplet interface, which serve the dual purpose of stabilizing the emulsion droplet and enabling future controlled release of drugs encapsulated in the nanoparticles. When injected into the suprachoroidal space of the eye with the cornea facing up, up to 50% of the injected PEDs were located in the most posterior quadrant of the suprachoroidal space near the macula. With the cornea facing down, approximately 59% of PEDs were located in the most anterior quadrant of the suprachoroidal space, near the ciliary body. Particles of approximately neutral density having similar size to PEDs did not show such targeting, consistent with gravity-mediated delivery. Larger PEDs (i.e., 35 μm diameter) were more effective at targeting than smaller PEDs. PEDs delivered to the back of the eye stayed there for at least 5 days. Measurements of suprachoroidal space closure kinetics suggest that the suprachoroidal space remained open for on the order of 1 min, providing a limited window of opportunity to move PEDs within the suprachoroidal space before it closes and entraps PEDs in place. This study shows for the first time that gravity-mediated delivery can be used to target the posterior and anterior regions of the suprachoroidal space of the eye to enable possible future treatments targeting the macula, ciliary body or other sites of therapeutic action.

5. Experimental Section

Microneedle fabrication

Metal microneedles were fabricated from 30-gauge needle cannulas (Becton Dickinson, Franklin Lakes, NJ). The cannulas were shortened to approximately 600-700 μm in length and the bevel at the orifice was shaped using a laser (Resonetics Maestro, Nashua, NH). The microneedles were electropolished using an E399 electropolisher (ESMA, South Holland, IL) and cleaned with deionized water, as shown in **Figure 8**.

Ex vivo injection procedure

Whole New Zealand White rabbit eyes (Pel-Freez Biologicals, Rogers, AR) with the optic nerve attached were shipped on ice and stored wet at 4°C for up to 2 days prior to use. Eyes were allowed to come to room temperature, and any fat and conjunctiva were removed to expose the sclera. A catheter was inserted through the optic nerve into the vitreous and connected to a bottle of Hank's Balanced Salt Solution (BSS, Corning Cellgro, Manassas, VA) raised to a height to generate internal eye pressure of 10 mmHg, which was used to mimic the lowered intraocular pressure in rabbit eyes under general anesthesia. The eye was positioned with cornea facing up or down, as needed to orient relative to gravity. The microneedle was attached to a gas-tight glass syringe containing the formulation to be injected. The microneedle was then inserted perpendicular to the sclera tissue 3 mm posterior from the limbus in the superior temporal quadrant of the eye. A volume of 200 μL was injected within 3 s and then an additional 30 s was allowed before removing the microneedle from the eye to prevent excessive reflux.

In vivo microneedle injection

Microneedle injection was done under systemic anesthesia (subcutaneous injection of a mixture of ketamine/xylazine/ace promazine at a dose of 17.5/8.5/0.5 mg/kg). Topical proparacaine (a drop of 0.5% solution) was given 2 - 3 min before microneedle injection as a local anesthetic. The rabbit was positioned with cornea facing up or down, as needed to orient relative to gravity. The microneedle was attached to a gas-tight glass syringe containing the formulation to be injected. For a suprachoroidal space injection, the eyelids of the rabbit were pushed back and the microneedle was inserted into the sclera 3 mm posterior to the limbus in the superior temporal quadrant of the eye. A volume of 200 μl was injected within 5 s and an additional 60 s was allowed before removing the microneedle from the eye to prevent excessive reflux. We maintained the animal in position and under anesthesia for 30 min after the injection to give enough time for the PEDs to completely settle down and all the aqueous formulation to dissipate out of the suprachoroidal space. At this point, if needed, an injection into the other eye was similarly performed. All experiments were carried out using New Zealand white rabbits with approval from the Georgia Tech Institutional Animal Care and Use Committee, and animals were euthanized with an injection of pentobarbital through the ear vein.

Particle-stabilized emulsion droplet formulation

Carboxylate-modified, nonbiodegradable, 200 nm diameter, fluorescent polystyrene nanoparticles at an initial concentration of 2% by weight (Fluospheres, Invitrogen, Carlsbad, CA) were diluted in BSS to obtain 0.6%, 0.4%, and 0.2% solutions. These solutions were then mixed at a 7:3 ratio by volume with perfluorocarbon (perfluorodecalin, Sigma-Aldrich, St. Louis, MO) and homogenized (PowerGen 700, Fisher Scientific, Pittsburgh, PA) at setting 5 for 20 s to form PEDs. The aqueous phase was then removed using pipettor and replaced with 1% polyvinyl alcohol (PVA, Sigma-Aldrich) in BSS solution. The solution was then filtered through various sizes (11, 20, 30, 40 μm) of nylon net filters (Millipore, Billerica MA) to obtain desired emulsion droplet sizes. Multiple images of the PEDs were taken using a microscope (IX 70, Olympus, Center Valley, PA) and the PED size

distribution was measured using ImageJ software (US National Institutes of Health, Bethesda, MD). The concentration of the PEDs was determined by the volume of settled PEDs per volume of aqueous phase (1% PVA). All the particle sizes were prepared using a concentration of 50 μl of PEDs per 1 mL of aqueous solution (1% PVA).

Tissue processing and measurement of fluorescent intensity

After the suprachoroidal injection, eyes were snap frozen in an isopropyl alcohol (2-isopropanol, Sigma Aldrich) bath, which was cooled in dry ice. After the eyes were completely frozen, they were removed and eight radial cuts were made from the posterior pole toward the anterior segment. After making eight cuts around the ocular globe, each "petal" was peeled away outwardly to expose the inside of the eye. This makes eyes into a flat mount-like "flower-petal" configuration visually exposing the inner side and the injected dyes in the eyes. Brightfield and fluorescence images of the inside of the eyes were imaged to visualize the distribution of fluorescent nanoparticles. Brightfield images were taken using a digital camera (Cannon Rebel T1i, Melville, NY) and fluorescence images were taken using a fluorescence microscope (Olympus SZX16, Center Valley, PA). Each of the eight petals was then divided into addi tional four pieces. Approximate distance from the ciliary body to the back of eye ranged from 1.2 - 1.4 mm. The cuts were made 3, 6, and 9 mm away from the ciliary body, where the suprachoroidal space starts, producing a total of 32 tissue pieces from each eye. Individual pieces were paired into 4 quadrants resulting in 16 vials each containing two pieces of the tissue in BSS solution. Ocular tissues were then homogenized (Fisher Scientific PowerGen) to extract injected nonbiodegradable fluorescent nanoparticles (**Figure S4** in Supplemental Information). The aqueous part of the mixture was pipetted out into 96 well plates to measure fluorescence signal intensity (Synergy Microplate Reader, Winooski, VT).

Particle-stabilized emulsion droplet fall time measurement

A solution containing 5% by volume PEDs was put into a clear glass vial and vigorously shaken before the start of recording the movement of PEDs using a digital camera (Cannon Rebel T1i). A green light bulb (Feit Electric, Pico Rivera, CA) was used to excite the fluorescent nanoparticles surrounding the PEDs and a red camera filter (Tiffen red filter, Hauppauge, NY) was mounted on the digital camera to visualize the movement of the PEDs. The height of the solution was measured and the time it took for essentially all the PEDs to fall to the bottom of the vial was measured.

Particle-stabilized emulsion droplet fall time modeling

The time it took for PEDs to fall to the bottom of the vial was modeled using the following equations[29].

$$F_{net}=F_g - F_B - F_D \quad (1)$$

$$\rho_o V_o x''(t)=\rho_o V_o g+\rho_f V_f g+6\pi\eta r x'(t) \quad (2)$$

Where F_{net} is the net force, F_g is gravitational force, F_B is buoyancy force, F_D is Stokes drag force, ρ_o is density of the PED (i.e., 1.9 g-cm^{-3}), ρ_f is density of a carrier fluid (i.e., water, 1 g-cm-3), V_o is the displacement volume of a PED (i.e. 1,440, 8,180, or 22,400 μm^3), V_f is the displacement volume of the carrier fluid (i.e., 1,440, 8,180, or 22,400 μm^3), g is gravitation acceleration (i.e., 9.8 m-s^{-2}), η is the viscosity of the carrier fluid (i.e., 1 cP), r is the radius of PED (i.e. 14, 25 or 35 μm), and $x(t)$ is height as a function of time.

Ultrasound measurement

An ultrasound scanner (UBM Plus, Accutome, Malvern, PA) was used to monitor the expansion of the suprachoroidal space. The injection was performed at a superior temporal site (between 1 and 2 o'clock) 3 mm back from the limbus and the ultrasound probe was positioned 45 degrees superior to the injection site (at 12 o'clock) 3 mm back from the limbus. Ultrasonic imaging was conducted before and for 10 min after the injection procedure.

Statistical Analysis

A minimum of three replicate experiments was performed for each treatment group, from which the mean and standard deviation were calculated. Experimental data were analyzed using one-way analysis of variance (ANOVA) to examine the difference between treatments. In all cases, a value of $p < 0.05$ was considered statistically significant.

Supplementary Material

Refer to Web version on PubMed Central for supplementary material.

Acknowledgments

We would like to thank Dr. Sven Behrens for helpful discussions and Donna Bondy for administrative support. This work was carried out at the Center for Drug Design, Development and Delivery and the Institute for Bioengineering and Bioscience at the Georgia Institute of Technology. This work was supported in part by the National Eye Institute (R24-EY017045 and R01-EY022097). Mark Prausnitz and Henry Edelhauser are inventors of patents that have been licensed to companies developing microneedle-based products, are paid advisors to companies developing microneedle-based products, and are founders/shareholders of companies developing microneedle-based products, including Clearside Biomedical. The resulting potential conflict of interest has been disclosed and is managed by Georgia Tech and Emory University.

References

1. Friedman DS, O'Colmain BJ, Munoz B, Tomany SC, McCarty C, de Jong PT, Nemesure B, Mitchell P, Kempen J. 2004; 122:564.Saaddine JB, Honeycutt AA, Narayan KM, Zhang X, Klein R, Boyle JP. Arch Ophthalmol. 2008; 126:1740. [PubMed: 19064858]
2. Chappelow AV, Kaiser PK. Drugs. 2008; 68:1029. [PubMed: 18484796] Peyman GA, Lad EM, Moshfeghi DM. Retina. 2009; 29:875. [PubMed: 19584648]
3. Bressler SB. Ophthalmology. 2009; 116:S1. [PubMed: 19800534] Janoria KG, Gunda S, Boddu SH, Mitra AK. Expert Opin Drug Deliv. 2007; 4:371. [PubMed: 17683251]
4. Nowak JZ. Pharmacological reports : PR. 2006; 58:353. [PubMed: 16845209] National Eye Institute. 2010
5. Ozkiris A, Erkilic K. Canadian journal of ophthalmology. Journal canadien d'ophtalmologie. 2005; 40:63.Jager, RD.; Aiello, LP.; Patel, SC.; Cunningham, ET, Jr.. Retina. Vol. 24. Philadelphia, Pa: 2004. p. 676

6. Patel SR, Lin AS, Edelhauser HF, Prausnitz MR. Pharm Res. 2011; 28:166. [PubMed: 20857178]
7. Olsen TW, Feng X, Wabner K, Csaky K, Pambuccian S, Cameron JD. Invest Ophthalmol Vis Sci. 2011; 52:4749. [PubMed: 21447680]
8. Olsen TW, Feng X, Wabner K, Conston SR, Sierra DH, Folden DV, Smith ME, Cameron JD. Am J Ophthalmol. 2006; 142:777. [PubMed: 16989764] Einmahl S, Savoldelli M, D'Hermies F, Tabatabay C, Gurny R, Behar-Cohen F. Invest Ophthalmol Vis Sci. 2002; 43:1533. [PubMed: 11980871] Gilger BC, Salmon JH, Wilkie DA, Cruysberg LP, Kim J, Hayat M, Kim H, Kim S, Yuan P, Lee SS, Harrington SM, Murray PR, Edelhauser HF, Csaky KG, Robinson MR. Invest Ophthalmol Vis Sci. 2006; 47:2596. [PubMed: 16723476]
9. Patel SR, Berezovsky DE, McCarey BE, Zarnitsyn V, Edelhauser HF, Prausnitz MR. Invest Ophthalmol Vis Sci. 2012; 53:4433. [PubMed: 22669719]
10. Verhoeven RS, VK.; Cacciamani, F.; Amar, T.; Yerxa, B. Association for Research in Vision and Ophthalmology. Seattle, WA: 2013. Edelhauser HF, MC.; Dean, R.; Powell, K.; Verhoeven, RS. Association for Research in Vision and Ophthalmology. Seattle, WA: 2013. Suprachoroidal Microinjection Delivers Triamcinolone Acetonide to Therapeutically-Relevant Posterior Ocular Structures and Limits Exposure in the Anterior Segment. Burke B, PS. Association for Research in Vision and Ophthalmology. Seattle, WA: 2013. Comparison of the Total Amount of Triamcinolone Acetonide Delivered Via Suprachoroidal or Intravitreal Administration.
11. Gilger BC, Abarca EM, Salmon JH, Patel S. Invest Ophthalmol Vis Sci. 2013; 54:2483. [PubMed: 23532526]
12. L. S. Morales-Canton, V.; Vera, RR.; Widmann, M.; Patel, SR.; Yerxa, B. Association for Research in Vision and Ophthalmology. Seattle, WA, M: 2013. Suprachoroidal Microinjection of Bevacizumab is Well Tolerated in Human Patients.
13. Kim YC, EH.; Prausnitz, MR. Association for Research in Vision and Ophthalmology. Seattle, WA: 2013.
14. Pickering SU. Journal of the Chemical Society. 1907; 91:2001. Transactions.
15. Aveyard R, Binks BP, Clint JH. Advances in Colloid and Interface Science. 2003:100–102. 503.
16. Edwards DA, Hanes J, Caponetti G, Hrkach J, Ben-Jebria A, Eskew ML, Mintzes J, Deaver D, Lotan N, Langer R. Science. 1997; 276:1868. [PubMed: 9188534] Arora S, Ali J, Ahuja A, Khar RK, Baboota S. AAPS PharmSciTech. 2005; 6:E372. [PubMed: 16353995]
17. Edwards DA, Ben-Jebria A, Langer R. Journal of applied physiology. 1998; 85:379. [PubMed: 9688708]
18. Kleinberg TT, Tzekov RT, Stein L, Ravi N, Kaushal S. Surv Ophthalmol. 2011; 56:300. [PubMed: 21601902]
19. Herzig EM, White KA, Schofield AB, Poon WCK, Clegg PS. Nat Mater. 2007; 6:966. [PubMed: 17982465]
20. Frelichowska J, Bolzinger MA, Chevalier Y. Journal of colloid and interface science. 2010; 351:348. [PubMed: 20800850]
21. Benz MS, Albini TA, Holz ER, Lakhanpal RR, Westfall AC, Iyer MN, Carvounis PE. Ophthalmology. 2006; 113:1174. [PubMed: 16647122]
22. Weinberger, D.; Goldenberg-Cohen, N.; Axer-Siegel, R.; Gaton, DD.; Yassur, Y. Retina. Vol. 18. Philadelphia, Pa: 1998. p. 233Haidt S, Clark L, Ginsberg J. Invest Ophthalmol Vis Sci. 1982; 22:233.
23. Liu Y, Miyoshi H, Nakamura M. Journal of controlled release. 2006; 114:89. [PubMed: 16824637]
24. Tambe DE, Sharma MM. Advances in Colloid and Interface Science. 1994; 52:1.
25. Miguel AS, Behrens SH. Soft Matter. 2011; 7:1948.
26. Edwards DA, Hanes J, Caponetti G, Hrkach J, BenJebria A, Eskew ML, Mintzes J, Deaver D, Lotan N, Langer R. Science. 1997; 276:1868. [PubMed: 9188534]
27. Atyabi F, Sharma HL, Mohammad HAH, Fell JT. Journal of Controlled Release. 1996; 42:105.
28. Peyman, S. A. M. Gholam A.; Conway, Mandi D. Vitreoretinal Surgical Techniques. Second Edition. Martin Dunitz; United Kingdom: 2001. Gross JG, Freeman WR, Goldbaum MH, Mendez TL. Br J Ophthalmol. 1989; 73:435. [PubMed: 2751976]
29. Bird, RB.; Stewart, WE.; Lightfoot, EN. Transport phenomena, J. New York. Wiley; 2002.

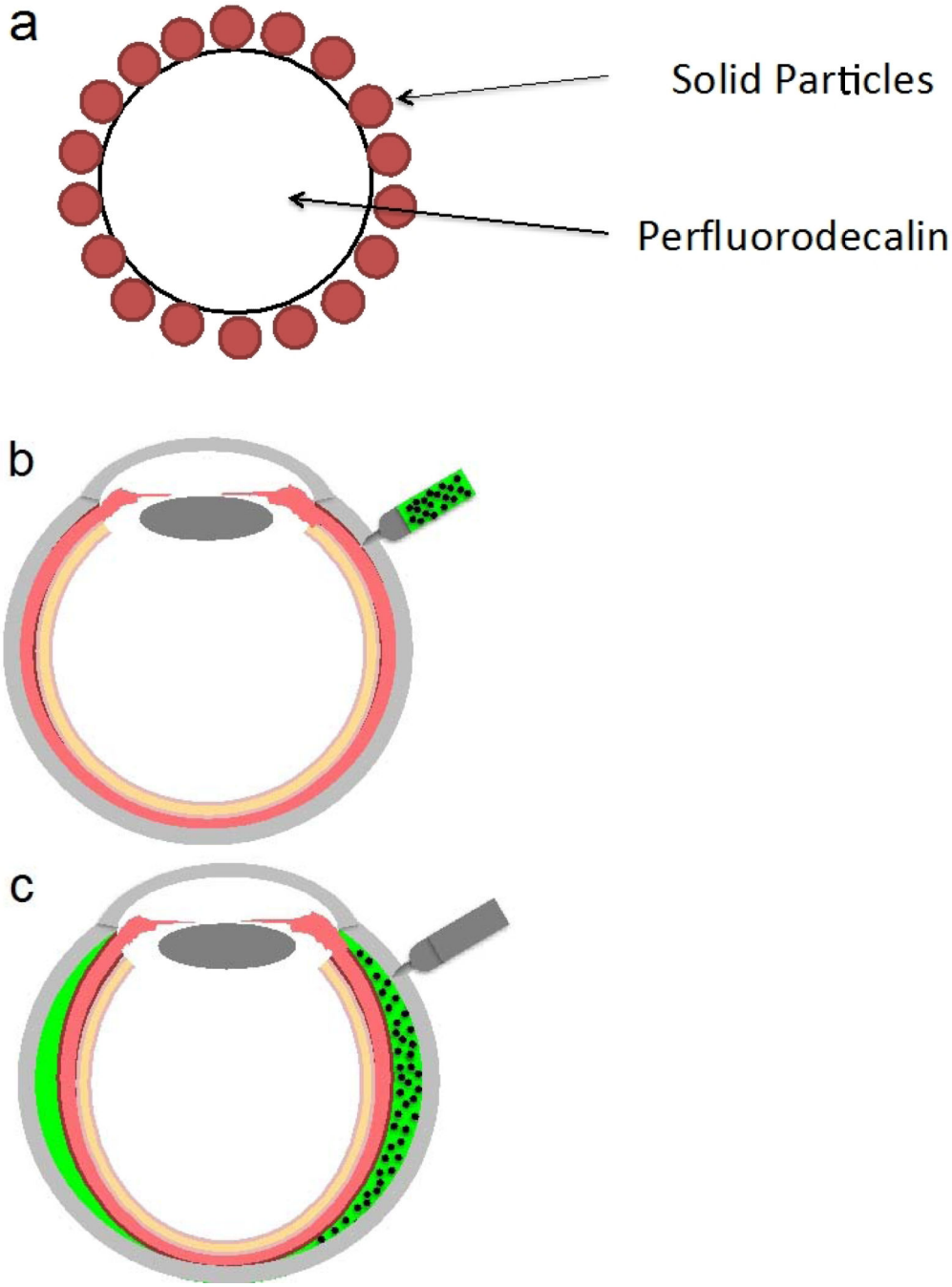

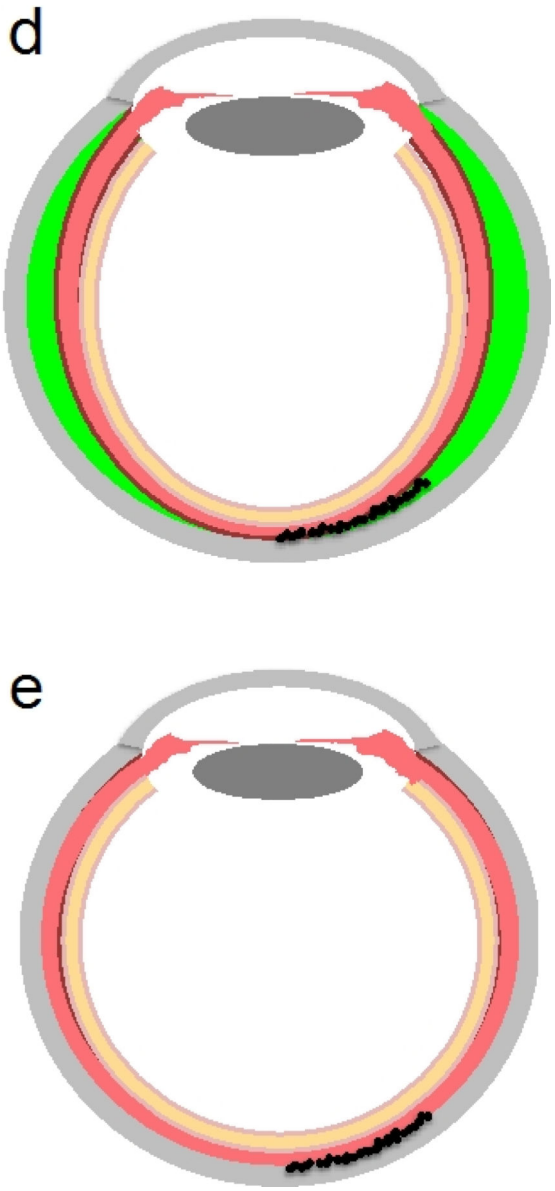

Figure 1.

Schematic diagram showing the design of PEDs. (a) The PED contains a perfluorodecaline liquid core, which has a density almost twice that of water. The surface of the PED is coated with polymeric nanoparticles, which stabilize the interface and serve as model particles to encapsulate drug for controlled release delivery. PEDS are designed to be injected into the suprachoroidal space of the eye (b), during which they initially distribute over a large area of the space (c), and then fall to the back of the eye due to gravity (d) and remain there after the aqueous carrier fluid is cleared (e).

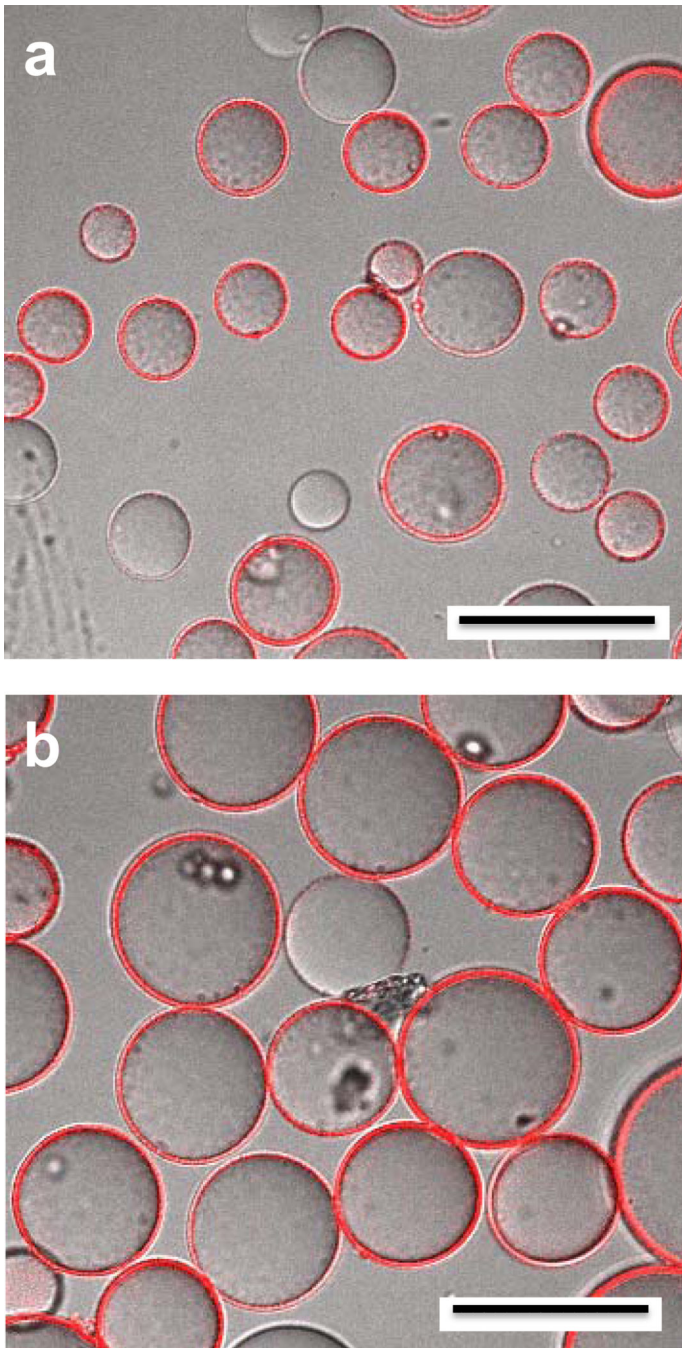

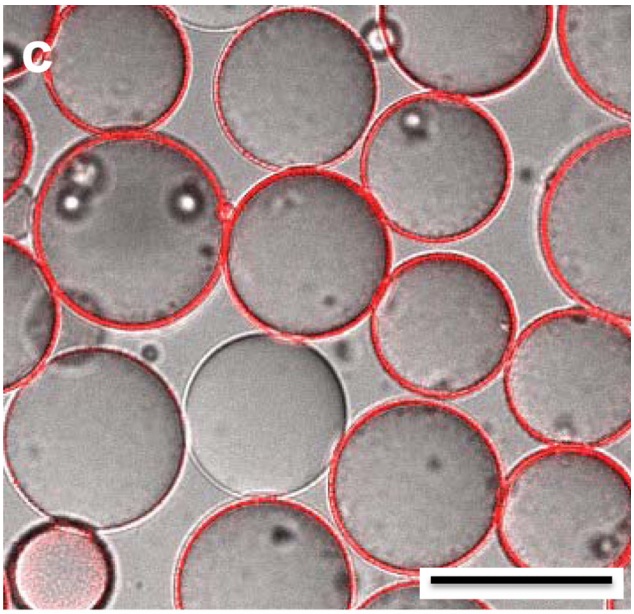

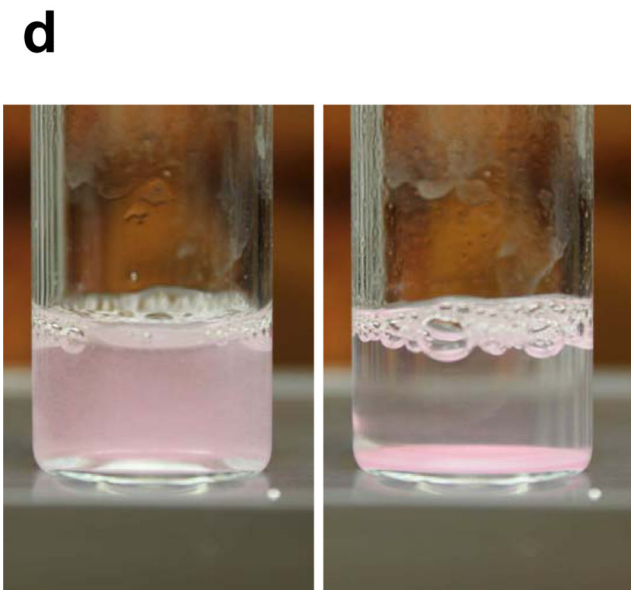

Figure 2.

Imaging of PEDs. Representative confocal microscope images of 14 μm (a), 25 μm (b), and 35 μm (c) diameter PEDs. The scale bar indicates 40 μm. Brightfield image of 35 μm PEDs immediately after vigorously shaking the vial (left) and 30 seconds later (right) (d).

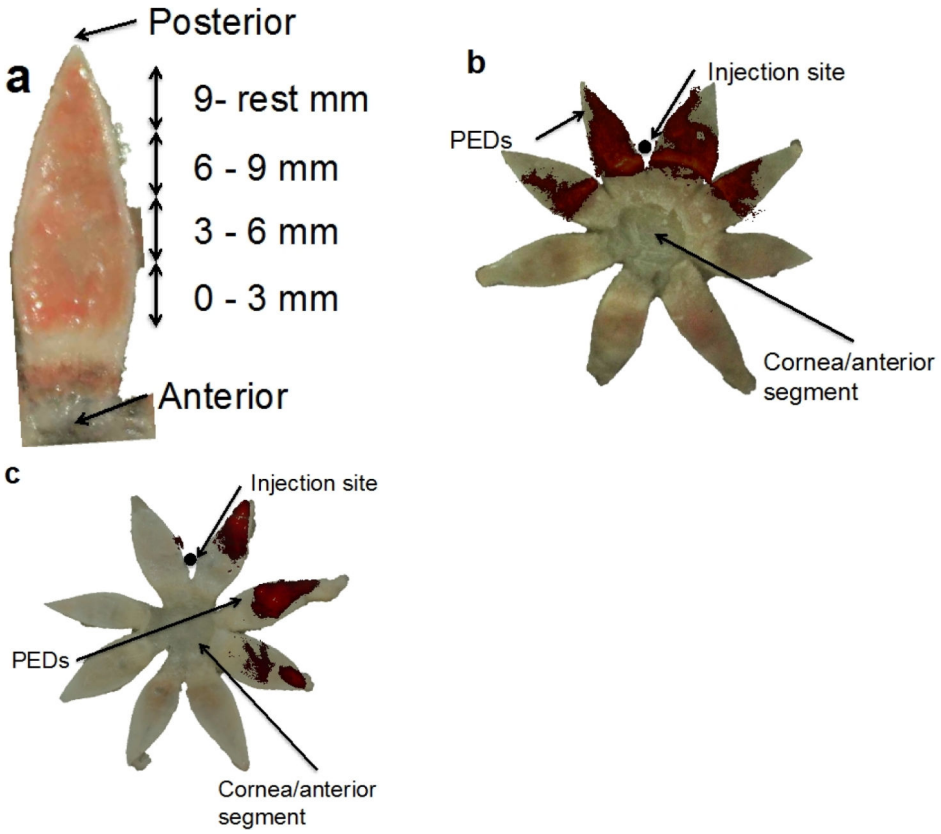

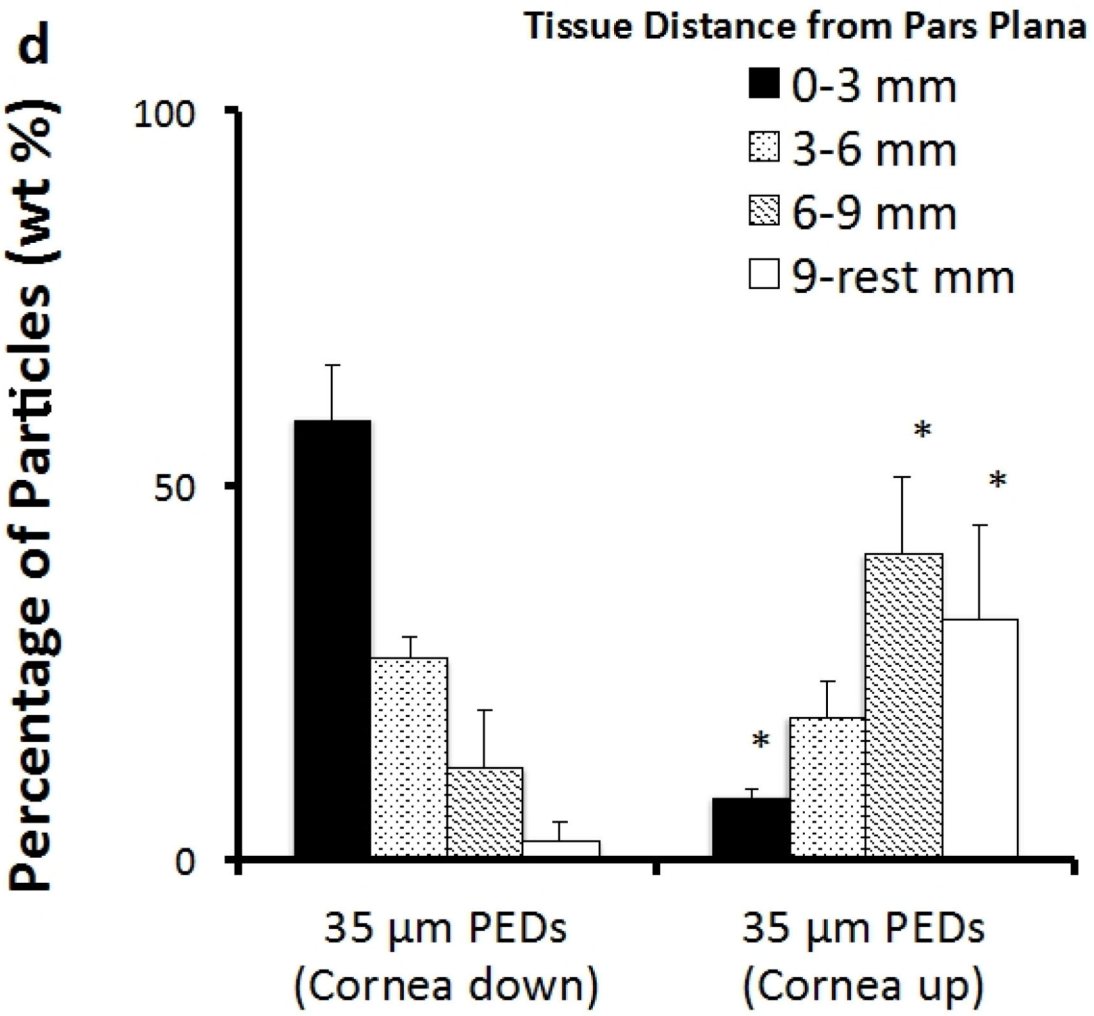

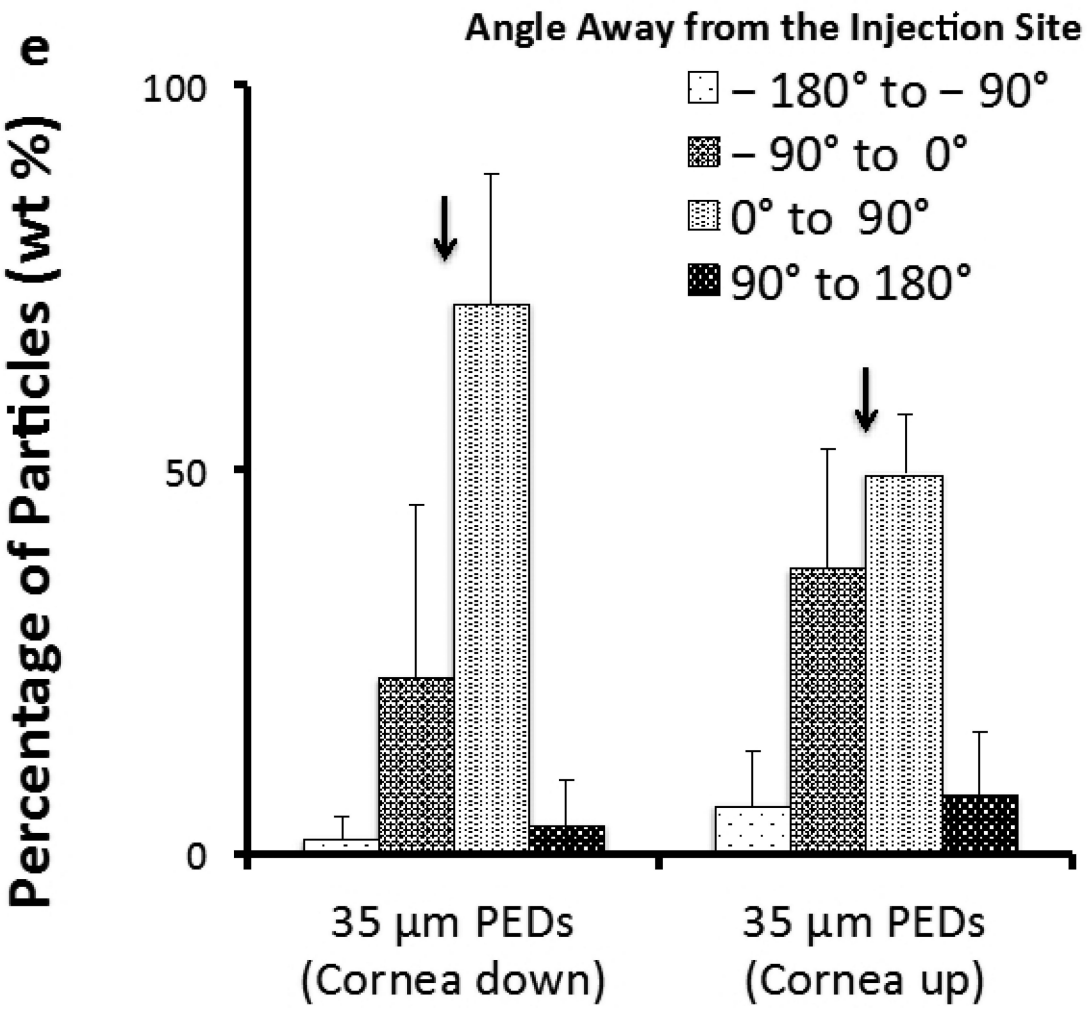

Figure 3.

Gravity-mediated delivery of PEDs in the rabbit eye *ex vivo*. (a) Representative image showing how each “petal” of dissected ocular tissue was subdivided for analysis into four antero-posterior quadrants, starting at the ciliary body and ending at the posterior pole. Representative images after injection of 35 μm-diameter PEDs into rabbit eyes showing localization to the (b) anterior and (c) posterior segment by changing orientation of the eye. In image (b), the cornea was oriented down during injection, whereas in image (c), the cornea was oriented up. The eyes were enucleated and frozen immediately after injection, after which they were cut open to form eight “petals” and the vitreous humor was removed. The eyes were then imaged by overlaying a brightfield microscopy image to show ocular anatomy with a fluorescence microscopy image of the same eye showing location of fluorescent nanoparticles. (d) Distribution of particles away from ciliary body for two different orientations (cornea down and up). (e) Radial distribution of particles away from the injection site (at superior “12-o'clock” position). The arrow indicates the injection site. Asterisk (*) indicates statistical significance between two different orientations. Data shown as average ± standard deviation (n = 3 – 5 replicates).

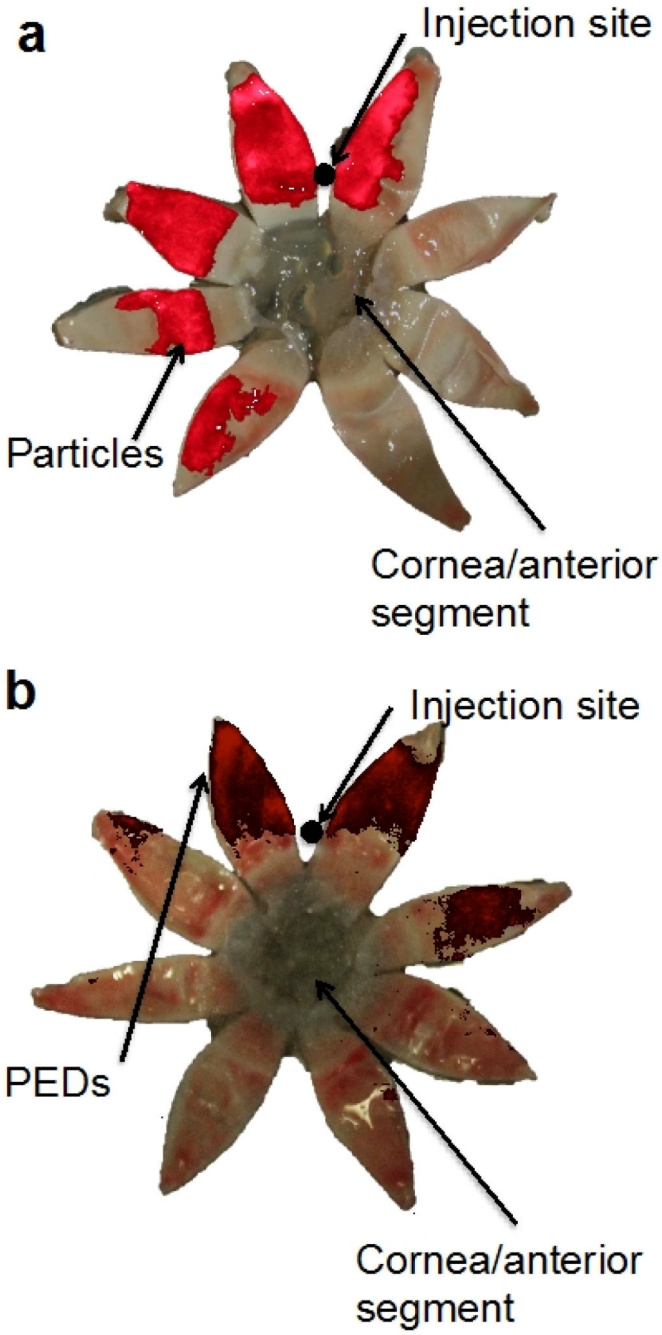

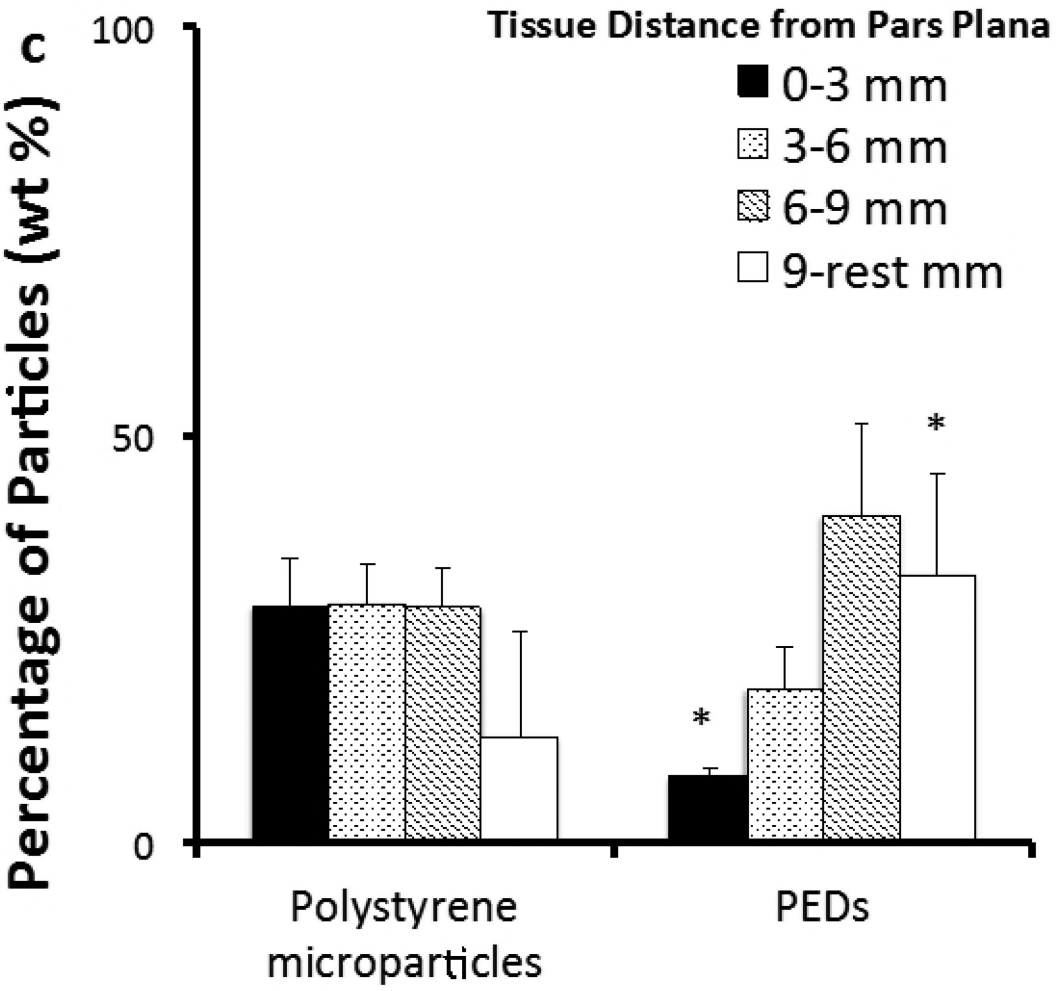

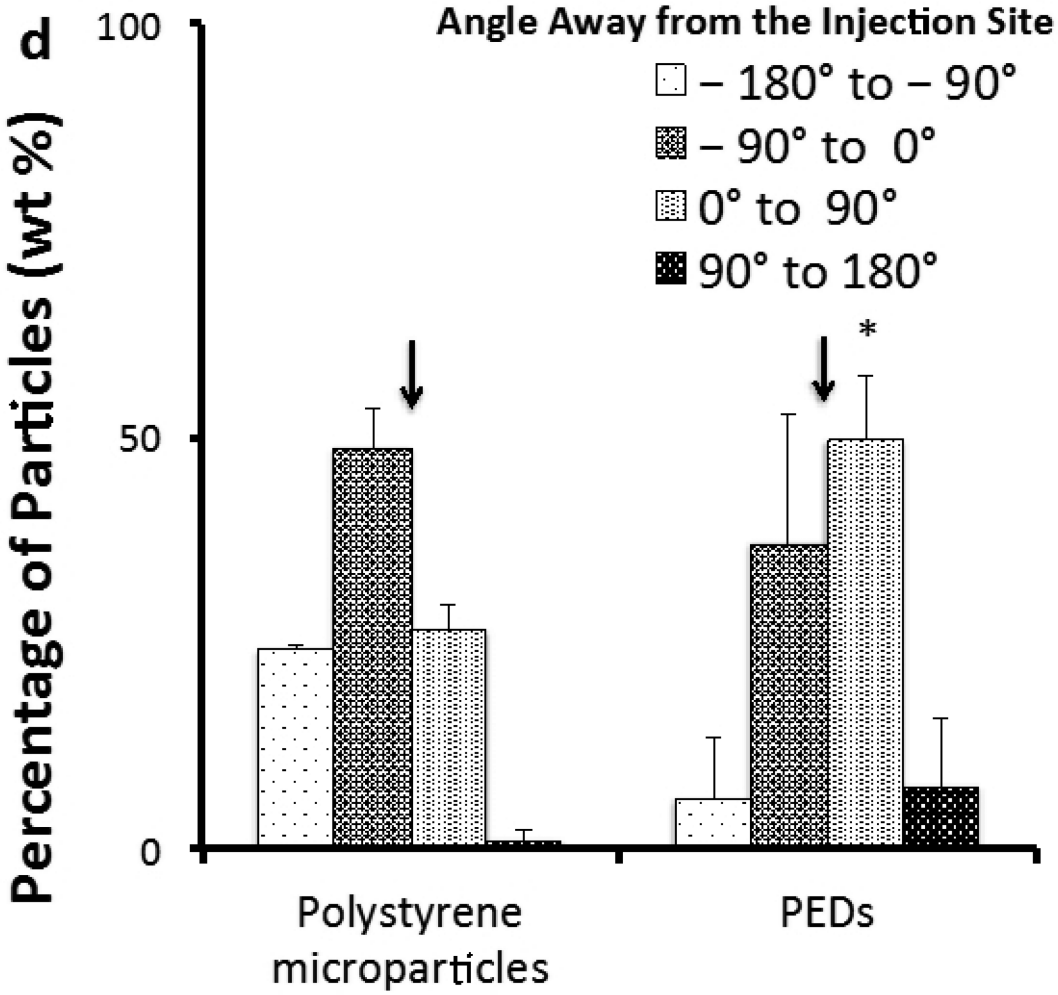

Figure 4.

Lack of effect of gravity on delivery of polystyrene microparticles in the rabbit eye *in vivo* (cornea facing up). (a) Distribution of almost-neutral density (1.05 g-cm^{-3}), 32 μm-diameter polystyrene microparticles after injection into the rabbit eye showing no preferential movement relative to gravity. (b) Distribution of high-density (1.92 g-cm^{-3}), 35 μm PEDs after injection into the rabbit eye showing gravity-mediated localization to the back of the eye. (c) Distribution of particles away from ciliary body and (d) radial distribution of particles away from the injection site (at superior “12-o'clock” position) for polystyrene microparticles and PEDs. The arrow indicates the injection site. Asterisk (*) indicates statistical significance between polystyrene microparticles and PEDs. Data shown as average ± standard deviation (n = 3).

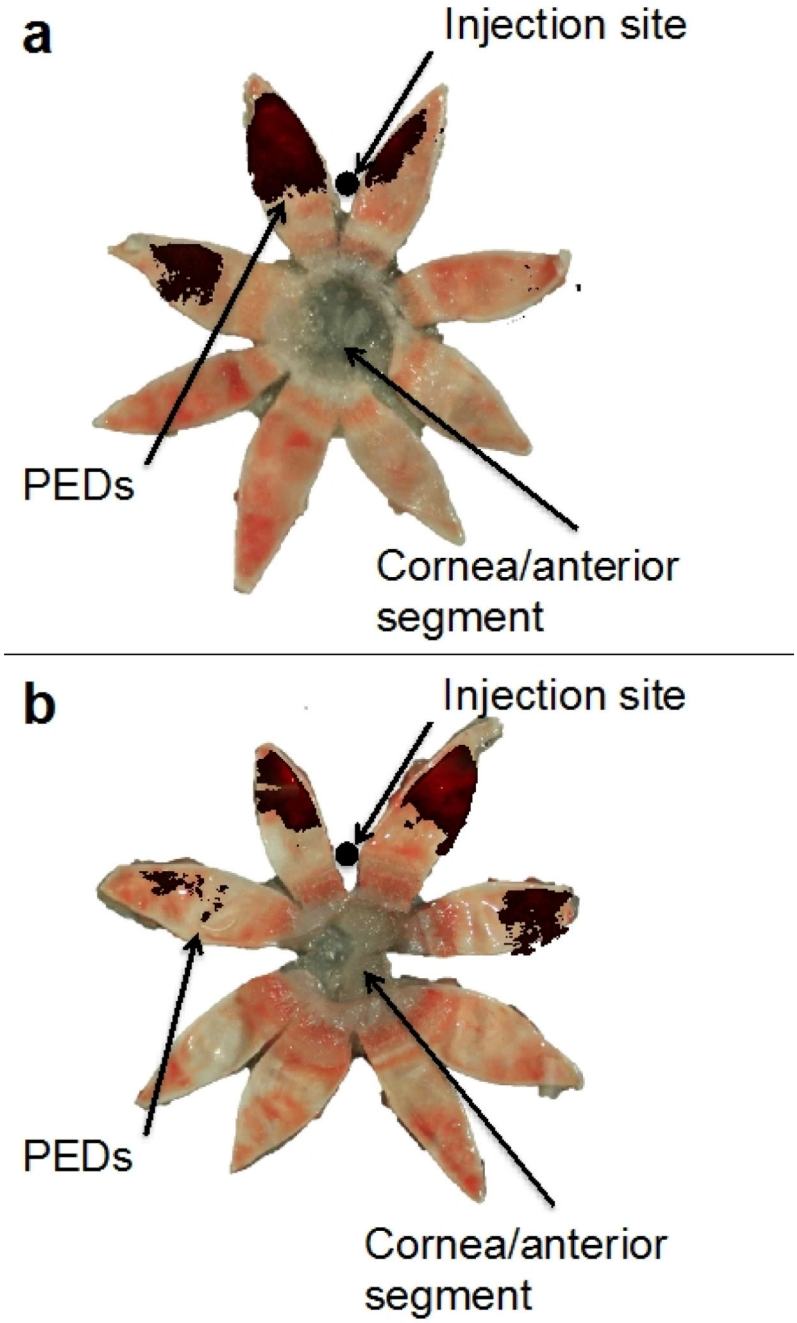

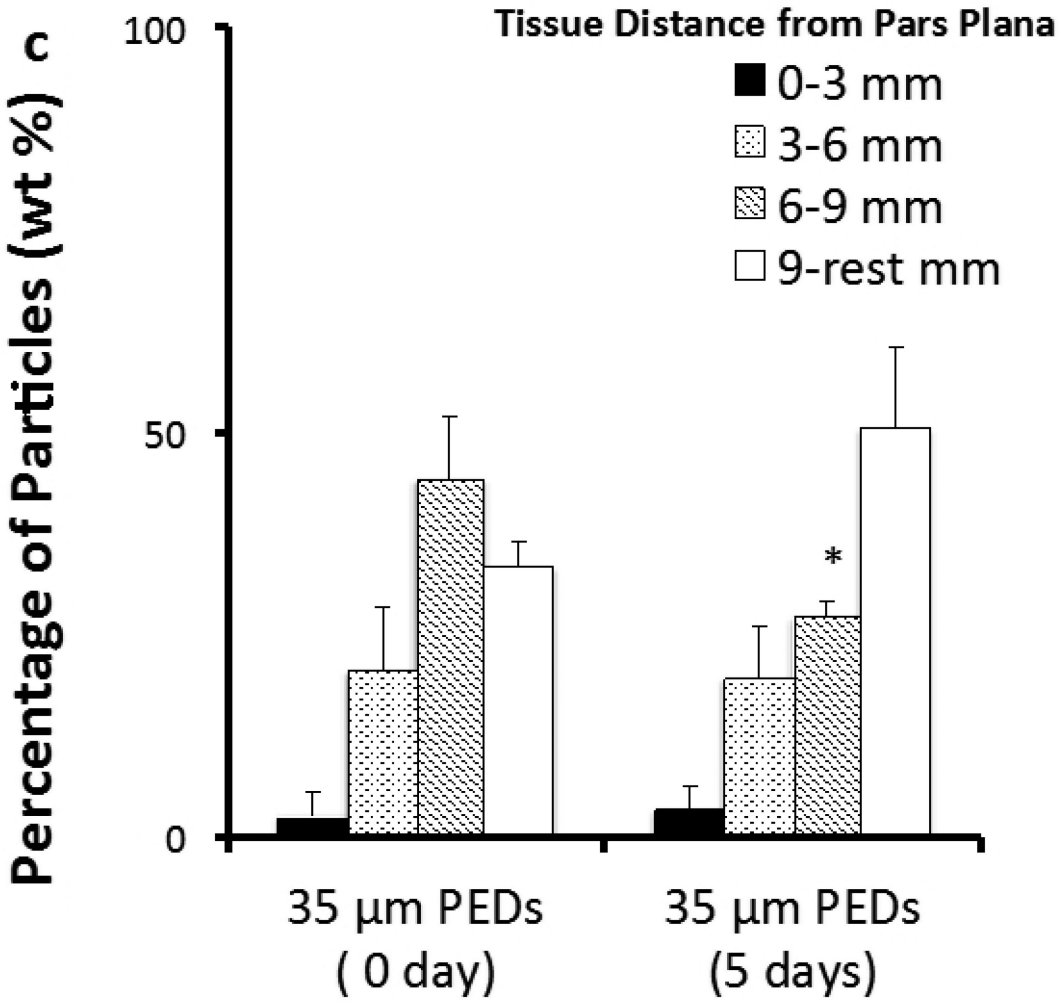

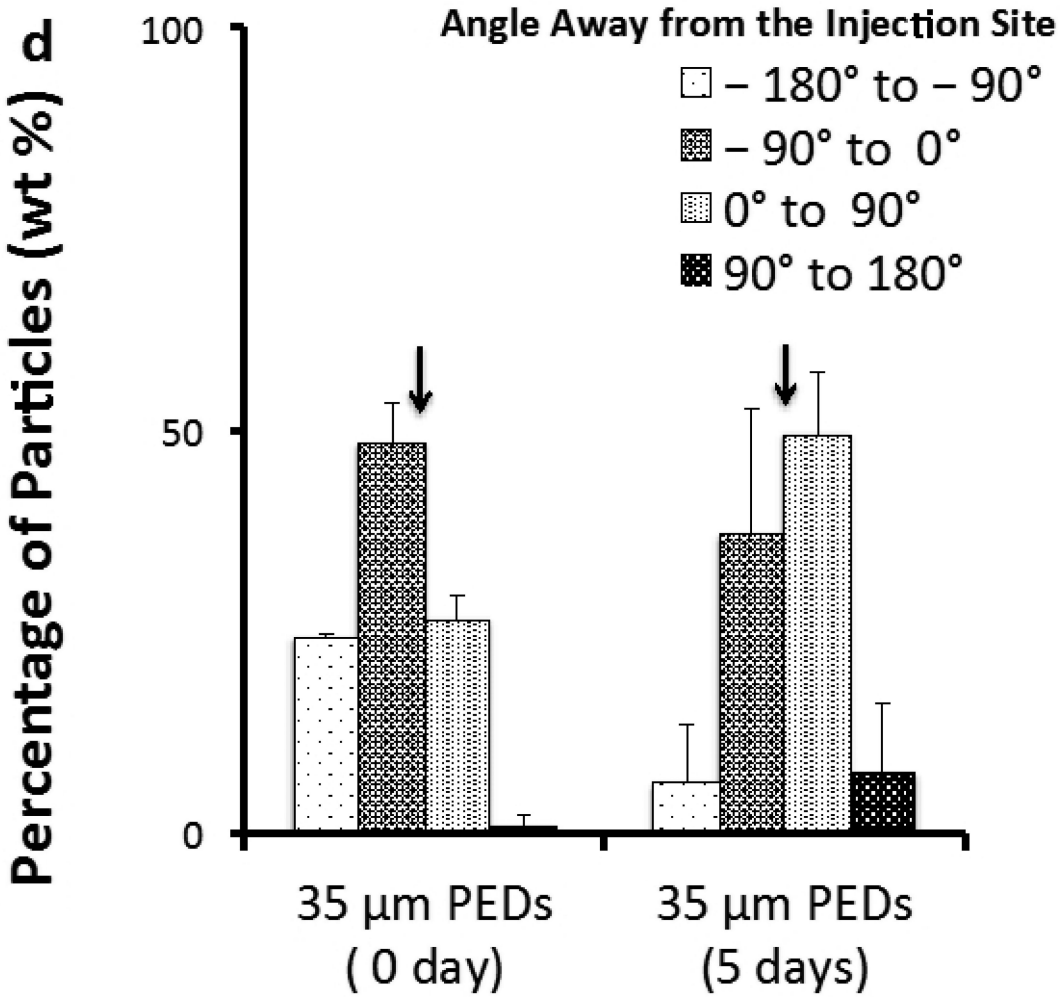

Figure 5.

Retention of PEDs at the site of targeted delivery. Distribution of PEDs (a) immediately after injection and (b) 5 days after injection in the rabbit eye *in vivo*. (c) Distribution of particles away from ciliary body and (d) radial distribution of particles away from the injection site (at superior “12-o'clock” position). The arrow indicates the injection site. Asterisk (*) indicates statistical significance between day 0 and day 5. Data shown as average ± standard deviation (n = 3).

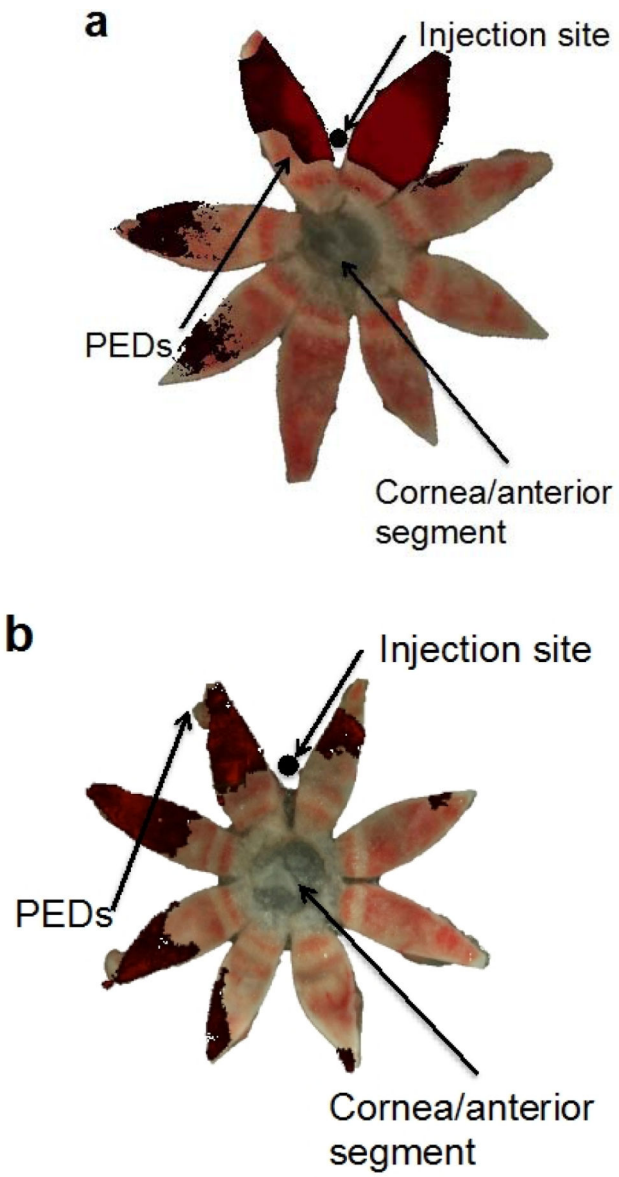

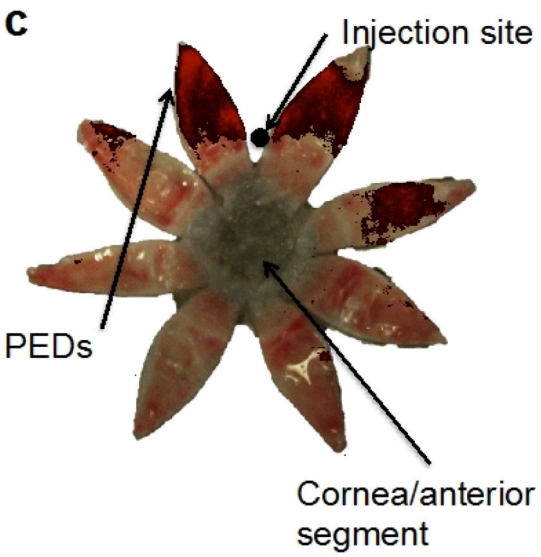

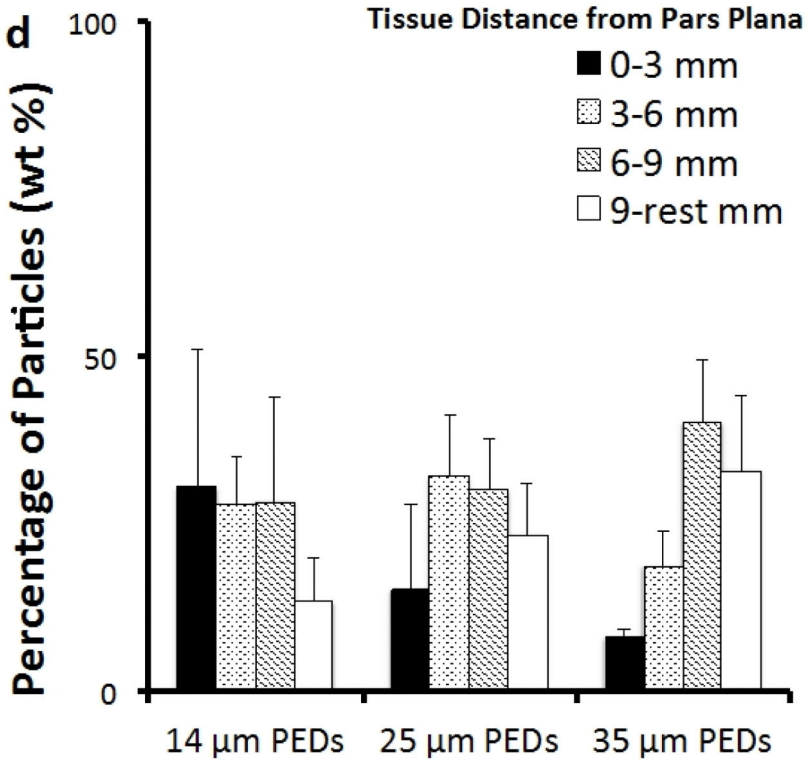

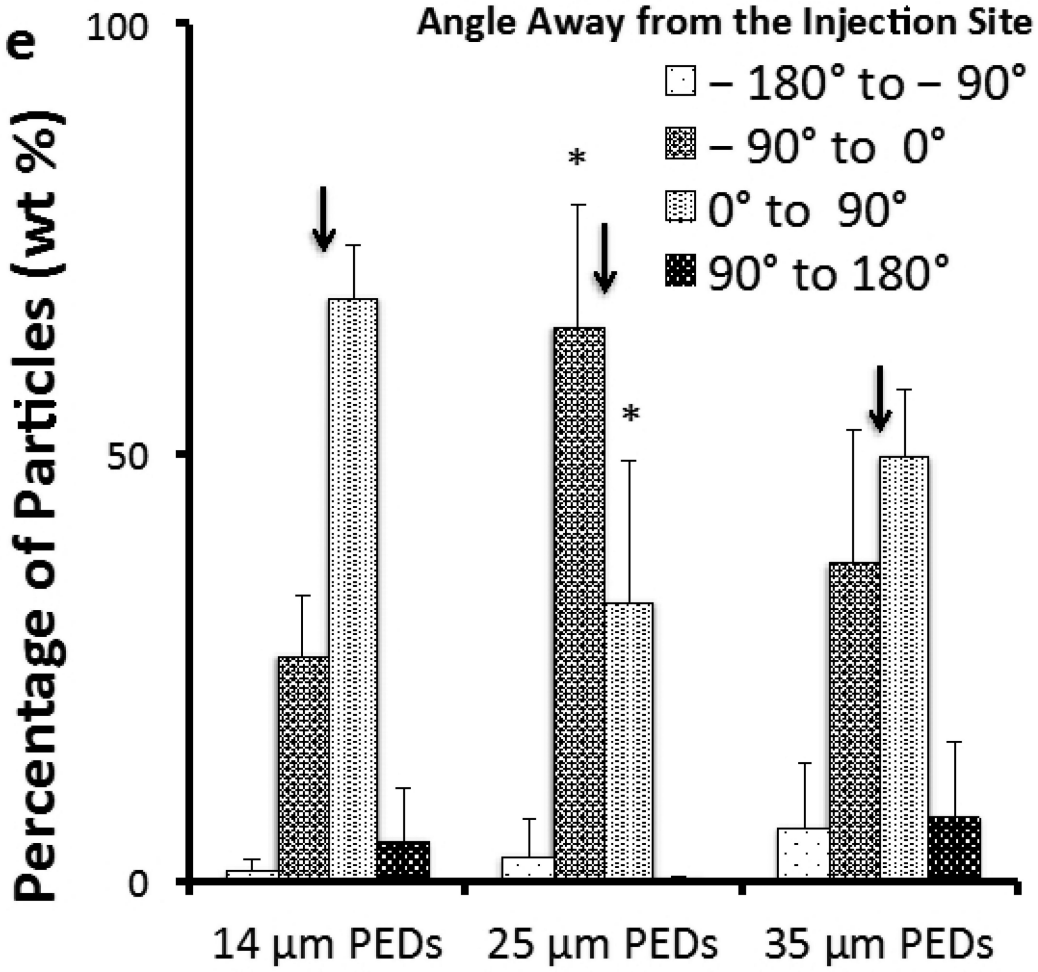

Figure 6.

Effect of PED size on gravity-mediated targeting. Distribution of PEDs of (a) 14, (b) 25 and (c) 35 μm diameter after injection in the rabbit eye *in vivo*. (d) Distribution of particles away from ciliary body and (e) radial distribution of particles away from the injection site (at superior “12-o'clock” position). The arrow indicates the injection site. Asterisk (*) indicates statistical significance between 14 μm and 25 μm PEDs. Data shown as average ± standard deviation (n = 3).

a

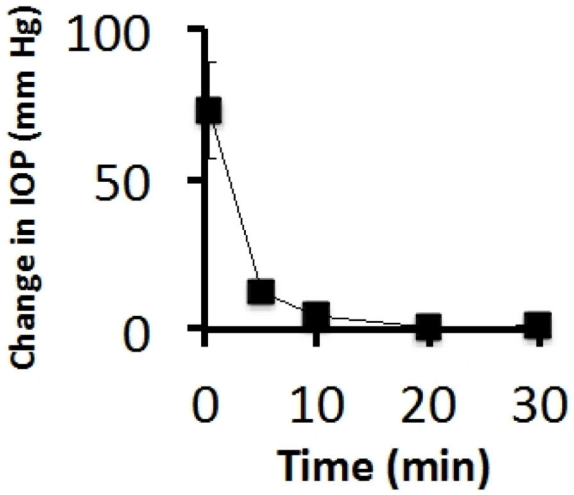

b

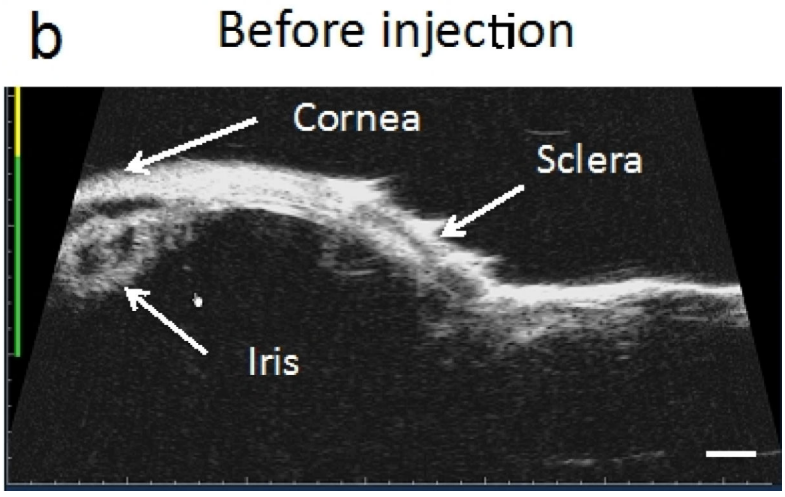

c 5 s. after injection

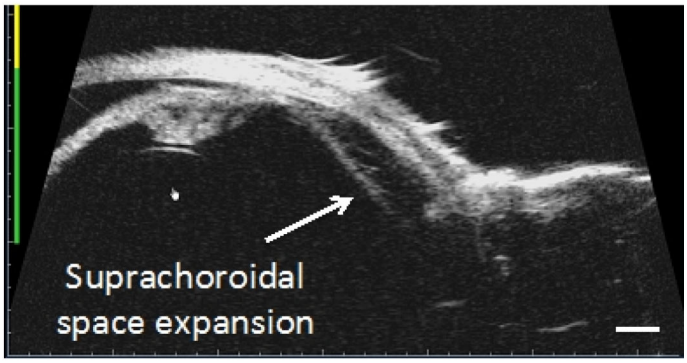

d 30 s. after injection

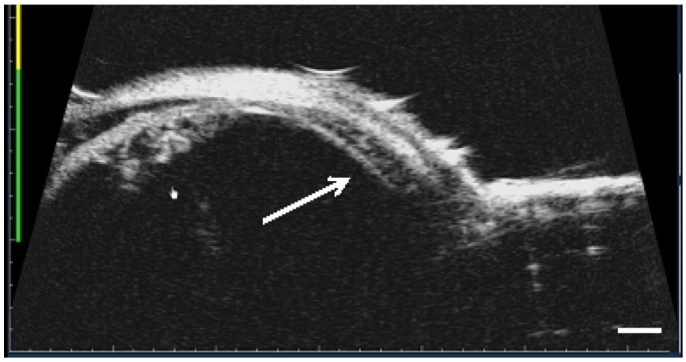

e 1 min. after injection

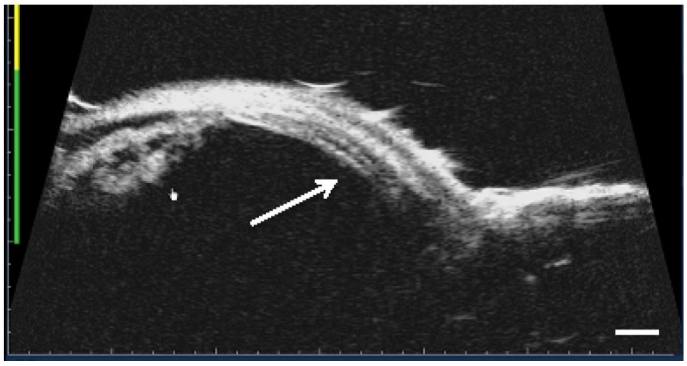

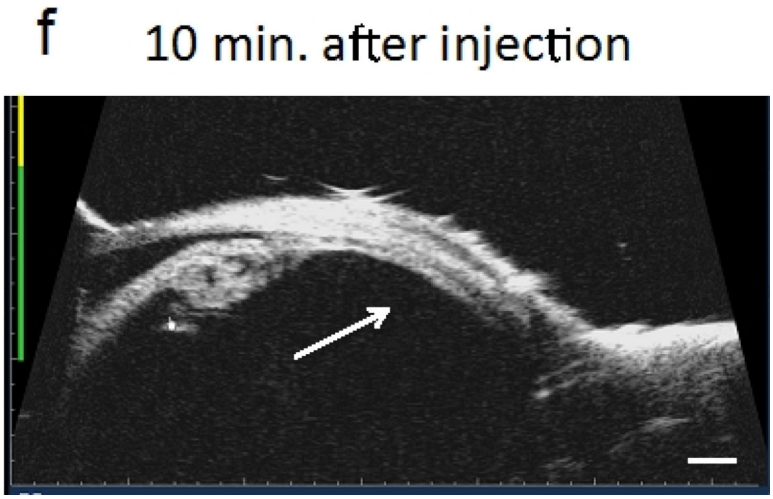

Figure 7.

Kinetics of suprachoroidal space collapse. (a) Intraocular pressure change after injecting 200 μl of BSS into the suprachoroidal space of the rabbit eye *in vivo*. Data shown as average ± standard deviation (n = 2). (b – f) Ultrasound images of the rabbit eye *in vivo* showing kinetics of the suprachoroidal space expansion and subsequent collapse after injecting 200 μl of BSS into suprachoroidal space. The injection was performed at a superior temporal site (between 1 and 2 o'clock) 3 mm back from the limbus and the ultrasound probe was positioned 45 degrees superior to the injection site (at 12 o'clock) 3 mm back from the limbus. The scale bar indicates 1 mm.

(a)

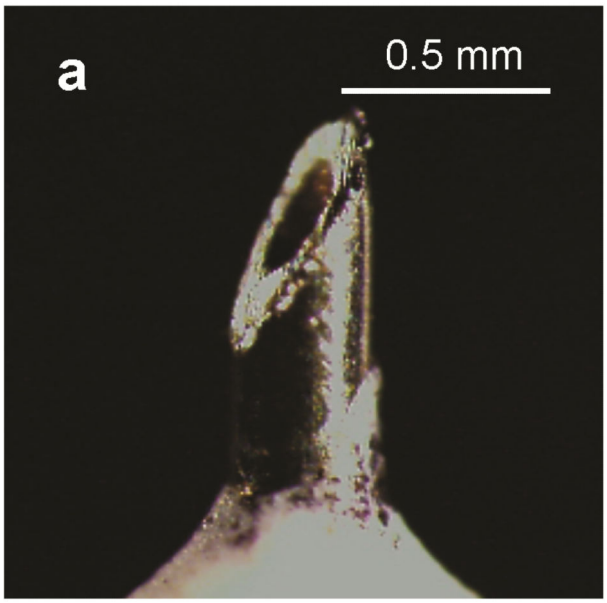

(b)

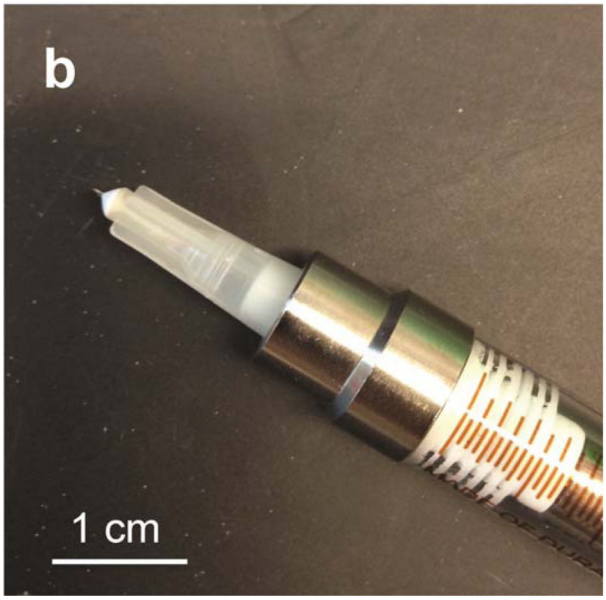

Figure 8.
Hollow microneedle (a) shown at high magnification and (b) mounted on a luer adapter attached to a syringe.